

## $\eta$ photoproduction and $N^*$ resonances

Ki-Seok Choi,<sup>1,\*</sup> Seung-il Nam,<sup>2,†</sup> Atsushi Hosaka,<sup>3,‡</sup> and Hyun-Chul Kim<sup>4,§</sup>

<sup>1</sup>*Department of Physics and Nuclear physics & Radiation Technology Institute (NuRI),  
Pusan National University, Busan 609-735, Korea*

<sup>2</sup>*Yukawa Institute for Theoretical Physics (YITP),  
Kyoto University, Kyoto 606-8502, Japan*

<sup>3</sup>*Research Center for Nuclear Physics (RCNP), Ibaraki, Osaka 567-0047, Japan*

<sup>4</sup>*Department of Physics, Inha University, Incheon 402-751, Korea*

(Dated: March, 2008)

### Abstract

We investigate the  $\eta$  photoproduction using the effective Lagrangian approach at the tree level. We focus on the new nucleon resonance  $N^*(1675)$ , which was reported by the GRAAL, CB-ELSA and Tohoku LNS, testing its possible spin and parity states theoretically ( $J^P = 1/2^\pm, 3/2^\pm$ ). In addition, we include six nucleon resonances,  $D_{13}(1520)$ ,  $S_{11}(1535)$ ,  $S_{11}(1650)$ ,  $D_{15}(1675)$ ,  $P_{11}(1710)$ ,  $P_{13}(1720)$  as well as the possible background contributions. We calculate various cross sections including beam asymmetries for the neutron and proton targets. We find noticeable isospin asymmetry in transition amplitudes for photon and neutron targets. This observation may indicate that the new resonance can be identified as a non-strangeness member of the baryon antidecuplet.

PACS numbers: 13.75.Cs, 14.20.-c

Keywords:  $\eta$  photoproduction, GRAAL experiment, Non-strangeness pentaquark

---

\*E-mail: kschoi@pusan.ac.kr

†E-mail: sinam@yukawa.kyoto-u.ac.jp

‡E-mail: hosaka@rcnp.osaka-u.ac.jp

§E-mail: hchkim@inha.ac.kr

## I. INTRODUCTION

After the first experimental report on the exotic baryon assigned as  $\Theta^+$  from the LESP collaboration at SPring-8 [1], there have been a large number of related experimental and theoretical works to date. Among them, the GRAAL collaboration reported a new nucleon resonance  $N^*(1675)$  from  $\eta$  photoproduction [2, 3]<sup>1</sup>. Their data show a narrow peak of which decay width  $\Gamma_{N^* \rightarrow \eta N}$  was estimated to be about 40 MeV. After the Fermi-motion correction being taken into account, the width may become even narrower  $\sim 10$  MeV [5]. This narrow width is a typical feature for the pentaquark exotic baryons [6, 7, 8]. Moreover, the production process of the  $N^*(1675)$  largely depends on its isospin state of the target nucleons: A larger  $N^*(1675)$  peak is shown for the neutron target, while it is suppressed for the proton one. Considering the fact that isospin-symmetry breaking is negligible at the strongly interacting vertex, this large asymmetry comes mainly from the photon coupling. Interestingly,  $N^*(1675)$  being assumed as a member of the baryon antidecuplet ( $\overline{10}$ ), this large isospin asymmetry was well explained in the chiral quark-soliton model ( $\chi$ QSM) [9, 10]. In fact, it originates from the  $U$ -spin conservation in the photon coupling [11]. This asymmetry was emphasized once again experimentally in Ref. [12]. Recently, the Tohoku LNS [13] and CB-ELSA [14] reported  $\eta$  photoproduction from the deuteron target, providing the same conclusion on that behavior. Concerning the spin and parity, their assignments are not yet determined unambiguously. Although the  $\eta$ -MAID has assumed  $J^P = 1/2^+$  as suggested by the  $\chi$ QSM [5], in our previous work [15], we have shown that  $J^P = 1/2^-$  was equally possible in comparison with the experimental data.

In the present work, following Ref. [15], we would like to present a recent study on the  $\eta$  photoproduction employing the effective Lagrangian approach in the Born approximation. We include six nucleon resonances  $D_{13}(1520)$ ,  $S_{11}(1535)$ ,  $S_{11}(1650)$ ,  $D_{15}(1675)$ ,  $P_{11}(1710)$ ,  $P_{13}(1720)$  in a fully relativistic manner. We ignore the contributions from  $N^*(1680, 5/2)$  and  $N^*(1700, 3/2)$  considered in Ref. [5] since their branching ratios to the  $\eta N$  channel are negligible. Nucleon pole terms and vector-meson exchanges are also taken into account as backgrounds. In order to test the spin and parity of the new resonance, we investigate the different four cases,  $J^P = 1/2^\pm, 3/2^\pm$ . We utilize the phenomenological form factors in terms of a gauge-invariant manner as done in Ref. [15, 16, 17]. As a result, we observe that  $\mu_{\gamma nn^*(1675)} = 0.1 \sim 0.2$  and  $\mu_{\gamma pp^*(1675)} \simeq 0$  for  $J^P = 1/2^\pm$  whereas  $\mu_{\gamma nn^*(1675)} = 0.01 \sim 0.02$  and  $\mu_{\gamma pp^*(1675)} \simeq 0$  for  $J^P = 3/2^\pm$  to reproduce the GRAAL data qualitatively well. Here,  $\mu_{\gamma NN^*(1675)}$  denotes the strengths of either magnetic or electric coupling between  $N$  and  $N^*(1675)$ . The present study seems to prefer the nucleon resonance of  $J^P = 1/2^\pm$ , but the possibility of higher spin can not be completely excluded.

The present work is organized as follows: In Section II, we provide our formalisms for  $\eta$  photoproduction. Differential cross sections and beam asymmetry being compared to the GRAAL data are given in Section III and Section IV, respectively, with discussions. Final section is devoted for summary and conclusion.

---

<sup>1</sup> Recent analysis has shown that the mass of the new resonance is about 1.68 GeV [4].

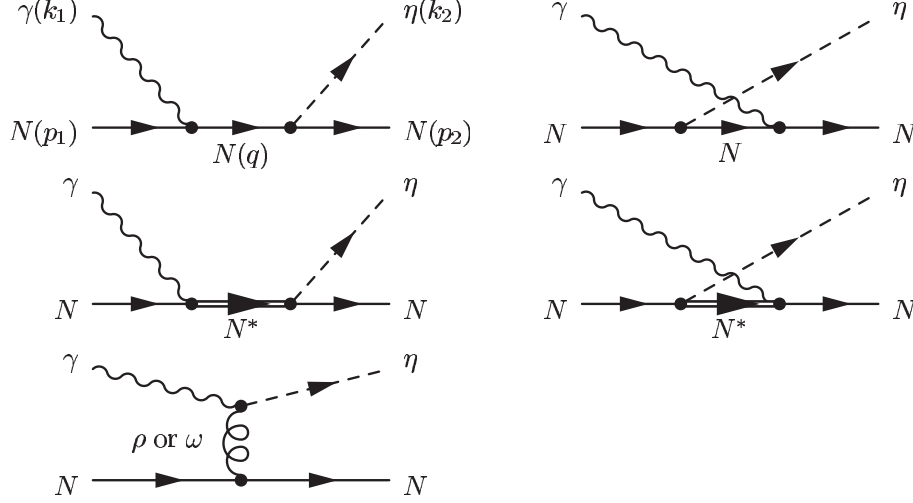


FIG. 1: Relevant tree-level diagrams for  $\eta$  photoproduction.

## II. FORMALISM

In this section, we present our model for  $\eta$  photoproduction. In Figure 1 we show the relevant tree-level diagrams for it schematically. The diagrams represent nucleon-pole (top) and resonance (middle) contributions in  $s$ - (left) and  $u$ -channels (right). In addition we also consider vector-meson exchanges ( $\rho$  and  $\omega$ ) in  $t$ -channel (bottom). The nucleon-pole and vector-meson exchange terms are assigned as the background contributions. The effective Lagrangians for the Yukawa vertices for the background contributions can be written as follows:

$$\begin{aligned}
\mathcal{L}_{\gamma NN} &= -e\bar{N}\not{A}N - i\frac{e\kappa_N}{2M_N}\bar{N}\sigma_{\mu\nu}q^\nu A^\mu N + \text{h.c.}, \\
\mathcal{L}_{\eta NN} &= -ig_{\eta NN}\bar{N}\gamma_5\eta N + \text{h.c.}, \\
\mathcal{L}_{VNN} &= -g_{VNN}^v\bar{N}\not{V}N - i\frac{g_{VNN}^t}{2M_N}\bar{N}\sigma_{\mu\nu}q^\nu V^\mu N + \text{h.c.}, \\
\mathcal{L}_{\gamma\eta V} &= \frac{eg_{\gamma\eta V}}{4M_\eta}\epsilon_{\mu\nu\sigma\rho}F^{\mu\nu}V^{\sigma\rho}\eta + \text{h.c.},
\end{aligned} \tag{1}$$

where  $\gamma$ ,  $N$ ,  $\eta$  and  $V$  stand for the fields of photon, nucleon,  $\eta$  meson and vector mesons ( $\rho$  and  $\omega$ ), respectively. The  $e$  and  $\kappa_N$  denote the electric charge and anomalous magnetic moment of the nucleon, respectively.  $M_h$  denotes the mass of the hadron  $h$ . The strength of the relevant couplings are employed from the Nijmegen potential model [18] as shown in Table I.

In the following we present the effective Lagrangians for the resonant contributions of

$g_{\eta NN}$	$g_{\rho NN}^v$	$g_{\rho NN}^t$	$g_{\omega NN}^v$	$g_{\omega NN}^t$	$g_{\rho\eta\gamma}$	$g_{\omega\eta\gamma}$
0.47	2.97	12.52	10.36	4.20	0.89	0.192

TABLE I: Strong and photon couplings for the background contributions.

spin 1/2, 3/2 and 5/2:

$$\begin{aligned}
\mathcal{L}_{\gamma NN^*}^{1/2} &= \frac{e\mu_{\gamma NN^*}}{2(M_N + M_{N^*})} \bar{N}^* \Gamma_5^a \sigma_{\mu\nu} F^{\mu\nu} N, \\
\mathcal{L}_{\gamma NN^*}^{3/2} &= \frac{ie\mu_{\gamma NN^*}}{M_{N^*}} \bar{N}^{*\mu} \Theta_{\mu\nu}(C, D) \Gamma_5^b \gamma_\lambda N F^{\lambda\nu}, \\
\mathcal{L}_{\gamma NN^*}^{5/2} &= \frac{e\mu_{\gamma NN^*}}{M_{N^*}^2} \bar{N}^{*\mu\alpha} \Theta_{\mu\nu}(E, F) \gamma_\lambda \Gamma_5^a (\partial_\alpha F^{\lambda\nu}) N, \\
\mathcal{L}_{\eta NN^*}^{1/2} &= -ig_{\eta NN^*} \bar{N} \Gamma \gamma_5 \eta N^*, \\
\mathcal{L}_{\eta NN^*}^{3/2} &= \frac{g_{\eta NN^*}}{M_\eta} \bar{N}^{*\mu} \Theta_{\mu\nu}(A, B) \Gamma_5^a N, \partial^\nu \eta \\
\mathcal{L}_{\eta NN^*}^{5/2} &= \frac{g_{\eta NN^*}}{m_\eta^2} \bar{N}^{*\mu\nu} \Theta_{\mu\delta}(A, B) \Theta_{\nu\lambda}(C, D) \Gamma_5^b N \partial^\delta \partial^\lambda \eta,
\end{aligned} \tag{2}$$

where the spinors for spin-3/2 and spin-5/2 fermions are defined by the Rarita-Schwinger formalism [19, 20] as given in Appendix. Moreover, as for the Lagrangians with the higher spins (3/2 and 5/2), it is necessary to take into account the off-shell parameter due to the point-transformation invariance [21]:

$$\Theta_{\mu\nu}(A, B) = g_{\mu\nu} + \left[ \frac{1}{2} (1 + 4B) A + B \right] \gamma_\mu \gamma_\nu. \tag{3}$$

Considering the gauge-invariance [22], we take  $A = -1$ , we can rewrite Eq. (3) as follows:

$$\Theta_{\mu\nu}(X) = g_{\mu\nu} + X \gamma_\mu \gamma_\nu, \quad X = -\left(B + \frac{1}{2}\right). \tag{4}$$

One can refer to the related topics for determining the off-shell parameters theoretically in Refs. [22, 23]. In the present work, we set the off-shell parameters to be zero for simplicity. This choice, however, is not bad, since resonance contributions become important only near their on-mass shells. The parity of the resonances are controlled by the matrices  $\Gamma_5^a$  and  $\Gamma_5^b$ :

$$\begin{aligned}
\text{Positive parity} &: \Gamma_5^a = \mathbf{1}_{4 \times 4}, \quad \Gamma_5^b = \gamma_5, \\
\text{Negative parity} &: \Gamma_5^a = \gamma_5, \quad \Gamma_5^b = \mathbf{1}_{4 \times 4}.
\end{aligned} \tag{5}$$

We determine the strengths of the strong couplings for the resonance of spin  $n/2$  ( $n = 1, 3, 5$ ) using the decay width  $\Gamma_{N^* \rightarrow \eta N}$  as input:

$$g_{\eta NN^*}^{n/2} = \left[ \frac{2(n+1) \pi M_{N^*} M_\eta^{n-1}}{\mathcal{C}_n^2 |\mathbf{P}_f|^n \left( \sqrt{M_N^2 + |\mathbf{P}_{\eta N}|^2} - \Pi \sin\left(\frac{n\pi}{2}\right) M_N \right)} \Gamma_{N^* \rightarrow \eta N} \right]^{\frac{1}{2}}, \tag{6}$$

$\mathcal{C}_n$  stands for the Clebsch-Gordan coefficient for the spin transition  $N \rightarrow N^*$  where  $\mathcal{C}_{1,3,5} = 1, \sqrt{2/3}, \sqrt{2/5}$ . The three momentum of the particles in the final state ( $\eta$  and  $N$ ),  $|\mathbf{P}_{h_1 h_2}|$  is defined by

$$|\mathbf{P}_{h_1 h_2}| = \left[ \left( \frac{M_{N^*}^2 - M_{h_1}^2 + M_{h_2}^2}{2M_{N^*}} \right)^2 - M_{h_2}^2 \right]^{\frac{1}{2}}. \tag{7}$$

The photon coupling to the resonances ( $\mu_{\gamma NN^*}$ ) can be computed by [19]:

$$\begin{aligned}
e\mu_{\gamma NN^*}^{1/2} &= \pm \left[ \frac{M_{N^*} M_N}{|\mathbf{P}_{\gamma N}|} \right]^{\frac{1}{2}} |A_{1/2}^{N^*}|, \\
e\mu_{\gamma NN^*}^{3/2} &= \pm S_{3/2}^{N^*} \sqrt{\frac{6M_N M_{N^*}^3}{(3M_{N^*}^2 + M_N^2) |\mathbf{P}_{\gamma N}|}} \left[ (A_{1/2}^{N^*})^2 + A_{3/2}^{N^*} \right]^{1/2} \\
e\mu_{\gamma NN^*}^{5/2} &= \mp S_{5/2}^{N^*} \sqrt{\frac{10M_N M_{N^*}^5}{(2M_{N^*} + M_N^2) |\mathbf{P}_{\gamma N}|^3}} \left[ (A_{1/2}^{N^*})^2 + (A_{3/2}^{N^*})^2 \right]^{1/2}.
\end{aligned} \tag{8}$$

Here, we account for the experimental fact that there is no strong correlation observed between  $A^{3/2}$  and  $A^{1/2}$ . Thus, we ignored the interference between them in Eq. (8). The sign of the coupling is determined by the dominant contribution using the following relations:

$$\begin{aligned}
S_{n/2}^{N^*} &= \text{sign}(A_{1/2}^{N^*}) \theta(h_{n/2}^{N^*}) + \text{sign}(A_{3/2}^{N^*}) \theta(-h_{n/2}^{N^*}), \\
h_{3/2}^{N^*} &= |A_{1/2}^{N^*}| - \frac{1}{\sqrt{2}} \frac{M_N}{M_{N^*}} |A_{3/2}^{N^*}|, \quad h_{5/2}^{N^*} = |A_{1/2}^{N^*}| - \frac{1}{\sqrt{3}} \frac{M_N}{M_{N^*}} |A_{3/2}^{N^*}|,
\end{aligned} \tag{9}$$

where  $\theta$  is the Heaviside step function. In Table II we list all phenomenological input for the strong and electromagnetic couplings for the relevant resonances in  $1.7 \text{ GeV} \lesssim E_{\text{cm}} \lesssim 1.9 \text{ GeV}$ . Note that all the strong coupling strengths are determined in order to reproduce the total and differential cross section data for the proton target [34] without the new resonance, since it was already shown in our previous work [15] that the contribution from  $p^*(1675)$  was negligible. We also fixed the photon couplings from the helicity amplitudes, listed in Table II [24]. However, as for  $F_{15}(1680)$ , we take relatively small values for the proton but large ones for the neutron, respectively, in order to obtain our numerical results compatible to the experimental data of Ref. [2, 3]. Note that we have excluded  $D_{13}(1700)$  considering its negligible branching ratio decaying to  $\eta N$ . We note that the branching ratio for  $D_{15}(1675)$  is much smaller than that used in the usual  $\eta$ -MAID analyses  $\sim 17\%$  [5]. We use  $\Gamma_{N^*(1675)} \simeq 40 \text{ MeV}$  and  $\Gamma_{N^*(1675)}/\Gamma_{N^*(1675) \rightarrow \eta N} \simeq 0.25$  for the new resonance as done in the previous work [15]. This choice is also equivalent to take the Fermi-motion correction into account, resulting in the smearing of the decay width [25].

The invariant amplitudes at the tree level can be evaluated straightforwardly using the effective Lagrangians given in Eqs. (1) and (2):

$$\begin{aligned}
i\mathcal{M}_s &= \frac{eg_{\eta NN}}{s - M_N^2} \bar{u}(p_2) \gamma_5 \left[ F_s^N \not{k}_1 + F_c(\not{p}_1 + M_N) + \frac{\kappa_N F_s^N}{2M_N} (\not{k}_1 + \not{p}_1 + M_N) \not{k}_1 \right] \not{p}_1 u(p_1), \\
i\mathcal{M}_u &= \frac{eg_{\eta NN}}{u - M_N^2} \bar{u}(p_2) \not{p}_2 \left[ F_c(\not{p}_2 + M_N) - F_s^N \not{k}_1 - \frac{\kappa_N F_u^N}{2M_N} \not{k}_1 (\not{p}_2 - \not{k}_1 + M_N) \right] \gamma_5 u(p_1), \\
i\mathcal{M}_t &= \frac{-ieg_{\eta NV} F_t^V \epsilon_{\mu\nu\sigma\rho}}{M_\eta (t - M_V^2)} \bar{u}(p_2) k_1^\mu \epsilon^\nu (k_1 - k_2)^\sigma \left[ g_{VNN}^V \gamma^\rho + \frac{g_{VNN}^t}{4M_N} [\not{p}_2 \gamma^\rho - \gamma^\rho (\not{k}_1 - \not{p}_1)] \right] u(p_1), \\
i\mathcal{M}_{s^*}^{1/2} &= \frac{e\mu_{\gamma NN^*} g_{\eta NN^*} F_s^{N^*}}{(M_N + M_{N^*}) [s - M_{N^*}^2 - iM_{N^*} \Gamma_{N^*}]} \bar{u}(p_2) \gamma_5 \Gamma_5^a (\not{k}_1 + \not{p}_1 + M_{N^*}) \Gamma_5^a \not{p}_1 u(p_1), \\
i\mathcal{M}_{s^*}^{3/2} &= -\frac{ieg_{\eta NN^*} \mu_{\gamma NN^*} F_s^{N^*}}{M_{N^*} M_\eta} \bar{u}(p_2) \Gamma_5^a D_{\mu\nu}^{3/2} k_2^\mu \Gamma_5^b \gamma_\sigma (k_1^\sigma \epsilon^\nu - k_1^\nu \epsilon^\sigma) u(p_1)
\end{aligned}$$

$N^*$	$\Gamma_{N^*}$	$\Gamma_{N^* \rightarrow \eta N} / \Gamma_{N^*}$	$A_{1/2}^{n^*}$	$A_{1/2}^{p^*}$	$A_{3/2}^{n^*}$	$A_{3/2}^{p^*}$
$D_{13}(1520)$	115	$2.3 \times 10^{-3}$	-0.059	-0.024	-0.139	0.166
$S_{11}(1535)$	130	55	-0.043	0.072	...	...
$S_{11}(1650)$	150	3	-0.041	0.037	...	...
$D_{15}(1675)$	165	0.05	-0.043	0.011	-0.058	0.006
$N^*(1675)$	40	25	...	...	...	...
$F_{15}(1680)$	130	1	0.080	-0.009	-0.040	0.015
$D_{13}(1700)$	100	0.025	0.00	-0.018	-0.003	-0.002
$P_{11}(1710)$	100	6.2	-0.002	0.009	...	...
$P_{13}(1720)$	200	4	0.001	0.010	0.029	-0.011

TABLE II: Relevant inputs for numerical calculations: full decay width [MeV], branching ratio [%] and helicity amplitude [ $\text{GeV}^{-1/2}$ ]. The new nucleon resonance is denoted by  $N^*(1675)$ .

$$\begin{aligned}
i\mathcal{M}_{s^*}^{5/2} &= -\frac{eg_{\eta NN^*}\mu_{\gamma NN^*}F_s^{N^*}}{M_\eta^2 M_{N^*}^2} \bar{u}(p_2) \Gamma_5^b k^{2\mu} k^{2\nu} D_{\mu\nu\rho\sigma}^{5/2} \gamma^\lambda \Gamma_5^a k^{1\rho} (k^{1\sigma} \epsilon_\lambda - k_{1\lambda} \epsilon^\sigma) u(p_1) \\
i\mathcal{M}_{u^*}^{3/2} &= -\frac{ieg_{\eta NN^*}\mu_{\gamma NN^*}F_u^{N^*}}{M_{N^*} M_\eta} \bar{u}(p_2) \Gamma_5^b \gamma_\sigma D_{\mu\nu}^{3/2} (k_1^\sigma \epsilon^\mu - k_1^\mu \epsilon^\sigma) \Gamma_5^a k_2^\nu u(p_1), \\
i\mathcal{M}_{u^*}^{1/2} &= \frac{e\mu_{\gamma NN^*} g_{\eta NN^*} F_u^{N^*}}{(M_N + M_{N^*}) [u - M_{N^*}^2 - iM_{N^*} \Gamma_{N^*}]} \bar{u}(p_2) \Gamma_5^a \not{k}_1 (\not{k}_2 - \not{p}_1 + M_{N^*}) \gamma_5 \Gamma_5^a u(p_1), \\
i\mathcal{M}_{u^*}^{5/2} &= -\frac{eg_{\eta NN^*}\mu_{\gamma NN^*}F_u^{N^*}}{m_\eta^2 M_{N^*}^2} \bar{u}(p_2) \gamma_\lambda \Gamma_5^a k_{1\nu} (k_1^\mu \epsilon^\lambda - k_1^\lambda \epsilon^\mu) D^{\mu\nu\sigma\rho} \Gamma_5^b k_{2\sigma} k_{2\rho} u(p_1), \tag{10}
\end{aligned}$$

where the Mandelstam variables are defined as  $s = (k_1 + p_1)^2$ ,  $s = (k_2 - p_1)^2$  and  $t = (k_1 - k_2)^2$ .  $D_{\mu\nu}^{3/2}$  and  $D_{\mu\nu\sigma\rho}^{5/2}$  denote the spin-3/2 and spin-5/2 propagators, respectively, in terms of the projections of the Rarita-Schwinger spinors (see Appendix):

$$\begin{aligned}
D_{\mu\nu}^{3/2} &\simeq \frac{\not{q} + M_{N^*}}{q^2 - M_{N^*}^2 - iM_{N^*} \Gamma_{N^*}} g_{\mu\nu}, \\
D_{\mu\nu\sigma\rho}^{5/2} &\simeq \frac{\not{q} + M_{N^*}}{q^2 - M_{N^*}^2 - iM_{N^*} \Gamma_{N^*}} \left[ \frac{1}{2} (T_{\mu\sigma} T_{\nu\rho} + T_{\mu\rho} T_{\nu\sigma}) \right], \\
T^{\mu\nu} &= -g^{\mu\nu} + \frac{q^\mu q^\nu}{M_{N^*}^2}. \tag{11}
\end{aligned}$$

where  $q$  designates the momentum of the resonance. As indicated in Ref. [16, 17], we use the simplified form for the spin-3/2 propagator as given in Eq. (11), since this form dominates the low energy region. Similarly, as for the spin-5/2 propagator, we consider the dominant contribution only.

Considering the extended structure of the hadrons ( $h$ ), we introduce a phenomenological form factor for the resonance and background contributions in a gauge-invariant manner [26, 27, 28, 29]:

$$F_x^h = \left[ \frac{\Lambda^4}{\Lambda^4 + (x - M_h^2)^2} \right]^m, \tag{12}$$

where  $x$  denotes the kinematical channel as well as the Mandelstem variables  $(s, u, t)$ . The power  $m$  is chosen to be unity for the spin-1/2 and -3/2 cases, and two for the spin-5/2 ones. This choice enables us to reduce unphysical behavior (monotonically increasing behavior beyond  $E_{\text{cm}} \sim M_{N^*}$ ) from the spin-5/2 propagator<sup>2</sup>. To satisfy gauge invariance and normalization condition of the form factor, we parameterize the form factor  $F_c$  as follows [26, 27, 28, 29]:

$$F_c = F_s^h + F_u^h - F_s^h F_u^h. \quad (13)$$

We note that the amplitudes for the vector-meson exchange and resonant contributions are gauge invariant. The cut-off masses are determined such that the data are well produced:

$$\Lambda_{N^*} = 0.9 \text{ GeV}, \Lambda_N = 0.8 \text{ GeV}, \Lambda_\rho = 0.8 \text{ GeV}, \Lambda_\omega = 1.2 \text{ GeV}, \quad (14)$$

### III. NUMERICAL RESULTS

In this Section, we provide numerical results for total and differential cross sections and beam asymmetries. First, we show those for the total cross sections as functions of the photon energy in the laboratory frame in Fig. 2 for the proton target (first and second rows) and neutron target (third and fourth rows). The results are shown separately for each spin-parity combination and the sign of  $\mu_{\gamma NN^*}$  ( $J_{\text{sign}}^P = 1/2_{\pm}^{\pm}$  and  $3/2_{\pm}^{\pm}$ ). When we turn off the effects from the new resonance ( $\mu_{\gamma pp^*} \approx 0$ ), the proton data are well reproduced. This tendency is well compatible with estimations from the  $\chi$ QSM [10] and consistent with our previous results [15]. On the contrary, as for the neutron target, we have varieties in the shapes of the curves due to the interferences between the new resonance and other contributions, depending on its spin, parity and sign( $\mu_{\gamma nn^*}$ ). We observe that there is constructive interference for the cases of  $J_{\text{sign}}^P = 1/2_+^+$ ,  $1/2_-^-$  and  $3/2_+^+$ , showing the peak due to the new resonance  $N^*(1675)$ . Note that the interference is mainly due to the new resonance and the spin-5/2 resonances,  $F_{15}(1680)$  and  $D_{15}(1675)$ . The absolute values of the photon coupling are found to be  $|\mu_{\gamma nn^*}| \geq 0.1$  for the spin-1/2 cases and  $|\mu_{\gamma nn^*}| \geq 0.01$  for the spin-3/2 ones, respectively, to provide clear peaks, indicating the evidence for the new resonance.

In Figs. 3 and 4, we draw the results for the differential cross sections as functions of  $\cos \theta$ , in which  $\theta$  stands for the angle between the incident photon and outgoing kaon in the center of mass (CM) frame, at a fixed photon energy  $E_\gamma = 800$  and 1145 MeV, where experimental data are available. At  $E_\gamma \approx 800$  MeV, which is almost the same with the threshold value, we have rather flat curves dominated by  $s$ -wave contributions as shown in Fig. 3. Especially, we can reproduce well the experimental data, taken from Refs. [34, 35], for the proton target case. The neutron results are also dominated by the  $s$ -wave ones and do not depend much on the spin and parity of the new resonance. As the photon energy increases, higher wave contributions start to come into play as shown in Fig. 4 for  $E_\gamma \approx 1145$  MeV. Again, the proton data are well reproduced. However, we have rather different shapes for the neutron showing a bump structure in the backward scattering region  $-1 \leq \cos \theta \leq -0.5$ . We verified

<sup>2</sup> We note that there have been several methods to remedy this unitarity breaking problem including the Blatt-Weisskopf penetration factor and introducing phenomenological off-shell parameters [19, 30, 31, 32].

that these bumps are due to the  $F_{15}(1680)$  contribution. Note that the dependence on  $J_{\text{sign}}^P$  is not so obvious again for all the spin-parity cases.

In Figs. 5 and 6, We show the differential cross sections with respect to the center of mass (CM) energy at fixed angle  $\theta = 140$  and  $65$  degrees, respectively. The experimental data for the neutron and proton targets are taken from Ref. [4]. Our results for the proton target slightly deviate from the data at  $\theta \approx 140^\circ$  as shown in Fig. 7, although the energy dependence beyond  $E_{\text{CM}} \approx 1750$  MeV, as well as the total cross section at the entire energy region are reproduced well. In contrast, the neutron data are well reproduced for the cases of  $J_{\text{sign}}^P = 1/2_+^+, 1/2_-^-$  and  $3/2_+^+$  as in the cases for the total cross section results. It turns out that  $|\mu_{\gamma nn^*}| \approx 0.1 \sim 0.2$  for the spin-1/2 cases and  $|\mu_{\gamma nn^*}| \approx 0.01 \sim 0.02$  for the spin-3/2 ones are appropriate to reproduce the observed peak. It is worth mentioning that, as for the  $J^P = 1/2^+$  case, the estimated value of  $|\mu_{\gamma nn^*}|$  is consistent with the result of the  $\chi$ QSM [10]. Focusing in the forward scattering region  $\theta \approx 65^\circ$  as shown in Fig. 6, our results for the proton target are overestimated in comparison to the experimental data. Interestingly, since the effects of  $F_{15}(1680)$  and  $D_{15}(1675)$  become stronger for the neutron target at this angle, the peak around  $E_{\text{CM}} \approx 1.7$  MeV becomes as high as that of  $S_{11}(1535)$ . Thus, it is not easy to find a clear evidence for the new resonance in the forward scattering region.

Finally, we would like to discuss the beam asymmetry for the present reaction process, which is defined as follows:

$$\Sigma = \left[ \frac{d\sigma}{d\Omega_{\parallel}} - \frac{d\sigma}{d\Omega_{\perp}} \right] \times \left[ \frac{d\sigma}{d\Omega_{\parallel}} + \frac{d\sigma}{d\Omega_{\perp}} \right]^{-1}. \quad (15)$$

Here the subscript  $\parallel$  denotes that the polarization vector of the incident photon is parallel to the reaction plane, and vice versa for  $\perp$ . From this definition, electric dominance of the photon coupling ( $E$ ) gives  $\Sigma \sim +1$  whereas magnetic one ( $M$ ) does  $\Sigma \sim -1$ . We show our results in Figs. 7 and 8 as functions of  $\theta$  at a fixed photon energy  $E_{\gamma} = 870$  and  $1051$  MeV for the same  $J_{\text{sign}}^P$ . In the vicinity of the threshold ( $E_{\gamma} \approx 870$  MeV), the proton data are well reproduced showing a positive bump at around  $\theta = 90^\circ$  which indicates that the electric photon coupling prevails. The bump structures are slightly shifted to the forward angle for the neutron target case, because of the effects from the spin-5/2 resonance contributions. However, from the beam asymmetry results, we can not see clear evidence for the new resonance. As the energy grows ( $E_{\gamma} \approx 1051$  MeV), the numerical results start to deviate from the experimental data for the proton as shown in Fig. 8; the theory is almost symmetric, while the experiment asymmetric and entitled to the forward scattering region. We consider that this deviation may result from unknown resonances, which are not taken into account here. Interestingly, although the results for the neutron are all similar to each  $J_{\text{sign}}^P$  case, the beam asymmetry becomes negative, resulting from the strong interference between the new resonance and  $F_{15}(1680)$ .

#### IV. SUMMARY AND CONCLUSION

We have investigated the  $\eta$ -meson photoproduction in an effective Lagrangian approach where the scattering amplitude was computed in the Born approximation. Following our previous work, we studied the role of the new nucleon resonance at round  $E_{\text{cm}} \sim 1.675$  GeV testing its possible spin and parity theoretically, considering  $1/2^\pm$  as well as  $3/2^\pm$ . In addition to this resonance, we considered six other nucleon resonances, i.e. ( $D_{13}(1520)$ ,



$S_{11}(1535)$ ,  $S_{11}(1650)$ ,  $D_{15}(1675)$ ,  $P_{11}(1710)$ ,  $P_{13}(1720)$ ), and nucleon-pole and vector-meson exchange contributions as backgrounds. All coupling strengths were determined by available experimental data and those obtained in the Nijmegen potential. Gauge invariance was satisfied explicitly via appropriate form factor schemes.

Total and differential cross sections were computed and compared with the experimental data. In general, the data for the proton were well reproduced without the new resonance contribution, while for the neutron data with that for  $J_{\text{sign}}^+ = 1/2_+^+$ ,  $1/2_-^+$  and  $3/2_-^+$ . Moreover, it turned out that the interferences between the new resonance and the spin-5/2 resonant contributions ( $F_{15}$  and  $D_{15}$ ) were crucial for the neutron target. We estimated  $|\mu_{\gamma nn^*}| \approx 0.1 \sim 0.2$  for the spin-1/2 cases and  $|\mu_{\gamma nn^*}| \approx 0.01 \sim 0.02$  for the spin-3/2 ones to reproduce the peak at  $E_{\text{CM}} \approx 1675$  MeV. However, it was not easy to determine the spin and parity of the new resonance unambiguously within the present framework.

From these observations, the new resonance can be considered as  $N^*(1/2^\pm, 3/2^+)$  along with the estimated strengths of  $\mu_{\gamma NN^*}$  at best in the present work. This is the same conclusion as in our previous work, in which the spin-3/2 cases were not taken into account. Among three possibilities of the spin and parity of  $N^*(1675)$ , it is interesting to adopt  $J^P = 1/2^+$ , since our reaction study implies a photon coupling which is consistent with the prediction of the chiral quark-soliton model. The photon coupling that vanishes for the proton resonance is a general consequence of SU(3) flavor symmetry when the resonance is identified as a member of the antidecuplet pentaquark baryons. Experimentally, we still need further information in order to establish that the peak structure in the deuteron target is the real one from the new resonance. Once it will be done, we will be able to make another step forward to exotic hadron spectroscopy.

## Acknowledgement

The authors are grateful to fruitful comments from J. K. Ahn, Y. Azimov, J. Kasagi, V. Kuznetsov, T. Nakano, H. Shimizu, and M. V. Polyakov. The present work is supported by the Korea Research Foundation Grant funded by the Korean Government(MOEHRD) (KRF-2006-312-C00507). The work of K.S.C. is partially supported by the Brain Korea 21 (BK21) project in Center of Excellency for Developing Physics Researchers of Pusan National University, Korea. The work of S.i.N. is supported in part by grant for Scientific Research (Priority Area No. 17070002) from the Ministry of Education, Culture, Science and Technology, Japan.

## Appendix

### A. Rarita-Schwinger vector-spinor

We can write the RS vector-spinors according to their spin states (3/2 and 5/2) as follows:

- Spin 3/2

$$u^\mu(p_2, \frac{3}{2}) = e_+^\mu(p_2)u(p_2, \frac{1}{2}),$$

$$u^\mu(p_2, \frac{1}{2}) = \sqrt{\frac{2}{3}}e_0^\mu(p_2)u(p_2, \frac{1}{2}) + \sqrt{\frac{1}{3}}e_+^\mu(p_2)u(p_2, -\frac{1}{2}),$$

$$\begin{aligned}
u^\mu(p_2, -\frac{1}{2}) &= \sqrt{\frac{1}{3}}e_-^\mu(p_2)u(p_2, \frac{1}{2}) + \sqrt{\frac{2}{3}}e_0^\mu(p_2)u(p_2, -\frac{1}{2}), \\
u^\mu(p_2, -\frac{3}{2}) &= e_-^\mu(p_2)u(p_2, -\frac{1}{2}).
\end{aligned} \tag{16}$$

• Spin 5/2

$$\begin{aligned}
u^{\mu\nu}(p_2, \frac{5}{2}) &= e_+^\mu e_+^\nu u(p_2, \frac{1}{2}), \\
u^{\mu\nu}(p_2, \frac{3}{2}) &= \sqrt{\frac{2}{5}}e_+^\mu e_0^\nu u(p_2, \frac{1}{2}) + \sqrt{\frac{1}{5}}e_+^\mu e_+^\nu u(p_2, -\frac{1}{2}) + \sqrt{\frac{2}{5}}e_0^\mu e_+^\nu u(p_2, \frac{1}{2}) \\
u^{\mu\nu}(p_2, \frac{1}{2}) &= \sqrt{\frac{1}{10}}e_+^\mu e_-^\nu u(p_2, \frac{1}{2}) + \sqrt{\frac{1}{5}}e_+^\mu e_0^\nu u(p_2, -\frac{1}{2}) \\
&\quad + \sqrt{\frac{2}{5}}e_0^\mu e_0^\nu u(p_2, \frac{1}{2}) + \sqrt{\frac{1}{5}}e_0^\mu e_+^\nu u(p_2, -\frac{1}{2}) + \sqrt{\frac{1}{10}}e_-^\mu e_+^\nu u(p_2, \frac{1}{2}) \\
u^{\mu\nu}(p_2, -\frac{1}{2}) &= \sqrt{\frac{1}{10}}e_+^\mu e_-^\nu u(p_2, -\frac{1}{2}) + \sqrt{\frac{1}{5}}e_0^\mu e_-^\nu u(p_2, \frac{1}{2}) \\
&\quad + \sqrt{\frac{2}{5}}e_0^\mu e_0^\nu u(p_2, -\frac{1}{2}) + \sqrt{\frac{1}{5}}e_-^\mu e_0^\nu u(p_2, \frac{1}{2}) + \sqrt{\frac{1}{10}}e_-^\mu e_+^\nu u(p_2, -\frac{1}{2}) \\
u^{\mu\nu}(p_2, -\frac{3}{2}) &= \sqrt{\frac{2}{5}}e_0^\mu e_-^\nu u(p_2, -\frac{1}{2}) + \sqrt{\frac{1}{5}}e_-^\mu e_-^\nu u(p_2, -\frac{1}{2}) + \sqrt{\frac{2}{5}}e_-^\mu e_0^\nu u(p_2, -\frac{1}{2}) \\
u^{\mu\nu}(p_2, -\frac{5}{2}) &= e_-^\mu e_-^\nu u(p_2, -\frac{1}{2}).
\end{aligned} \tag{17}$$

Here, we employ the basis four-vectors  $e_\lambda^\mu$  which reads:

$$\begin{aligned}
e_\lambda^\mu(p_2) &= \left( \frac{\hat{e}_\lambda \cdot \mathbf{p}_2}{M_B}, \hat{e}_\lambda + \frac{\mathbf{p}_2(\hat{e}_\lambda \cdot \mathbf{p}_2)}{M_B(p_2^0 + M_B)} \right), \\
\hat{e}_+ &= -\frac{1}{\sqrt{2}}(1, i, 0), \quad \hat{e}_0 = (0, 0, 1), \quad \hat{e}_- = \frac{1}{\sqrt{2}}(1, -i, 0).
\end{aligned} \tag{18}$$

- 
- [1] T. Nakano *et al.* [LEPS Collaboration], Phys. Rev. Lett. **91**, 012002 (2003).  
[2] V. Kuznetsov [GRAAL Collaboration], arXiv:hep-ex/0409032.  
[3] V. Kuznetsov [GRAAL Collaboration], arXiv:hep-ex/0606065.  
[4] V. Kuznetsov *et al.*, Phys. Lett. B **647**, 23 (2007).  
[5] A. Fix, L. Tiator and M. V. Polyakov, arXiv:nucl-th/0702034.  
[6] D. Diakonov and V. Petrov, Phys. Rev. D **69**, 094011 (2004).  
[7] R. A. Arndt, Y. I. Azimov, M. V. Polyakov, I. I. Strakovsky and R. L. Workman, Phys. Rev. C **69**, 035208 (2004).  
[8] M. V. Polyakov and A. Rathke, Eur. Phys. J. A **18**, 691 (2003).  
[9] Y. Azimov, V. Kuznetsov, M. V. Polyakov and I. Strakovsky, Eur. Phys. J. A **25**, 325 (2005).  
[10] H. -Ch. Kim, M. V. Polyakov, M. Praszalowicz, G. S. Yang and K. Goeke, Phys. Rev. D **71**, 094023 (2005).

- [11] A. Hosaka, talk given at the international conference Baryons07, Seoul, Korea.
- [12] V. Kuznetsov, M. V. Polyakov, T. Boiko, J. Jang, A. Kim, W. Kim and A. Ni, arXiv:hep-ex/0703003.
- [13] J. Kasagi, talk given at the international workshop YKIS06 in Kyoto, Japan.
- [14] B. Krusche *et al.*, talk given at the international workshop QNP06, Madrid, Spain.
- [15] K. S. Choi, S. i. Nam, A. Hosaka and H. -Ch. Kim, Phys. Lett. B **636**, 253 (2006).
- [16] S. i. Nam, A. Hosaka and H. -Ch. Kim, Phys. Rev. D **71**, 114012 (2005).
- [17] S. i. Nam, A. Hosaka and H. -Ch. Kim, Phys. Lett. B **633**, 483 (2006).
- [18] V. G. J. Stoks and T. A. Rijken, Phys. Rev. C **59**, 3009 (1999).
- [19] A. I. Titov and T. S. H. Lee, Phys. Rev. C **66**, 015204 (2002).
- [20] W. Rarita and J. S. Schwinger, Phys. Rev. **60**, 61 (1941).
- [21] B. J. Read, Nucl. Phys. B **52**, 565 (1973).
- [22] L. M. Nath, B. Etemadi and J. D. Kimel, Phys. Rev. D **3**, 2153 (1971).
- [23] J. D. Kimel and L. M. Nath, Phys. Rev. D **6**, 2132 (1972).
- [24] W. M. Yao *et al.* [Particle Data Group], J. Phys. G **33**, 1 (2006).
- [25] Y. Azimov, private communication.
- [26] K. Ohta, Phys. Rev. C **40**, 1335 (1989).
- [27] H. Haberzettl, C. Bennhold, T. Mart and T. Feuster, Phys. Rev. C **58**, 40 (1998).
- [28] R. M. Davidson and R. Workman, Phys. Rev. C **63**, 025210 (2001).
- [29] S. i. Nam, A. Hosaka and H. -Ch. Kim, J. Korean Phys. Soc. **49**, 1928 (2006).
- [30] M. Post, S. Leupold and U. Mosel, Nucl. Phys. A **689**, 753 (2001).
- [31] D. M. Manley and E. M. Saleski, Phys. Rev. D **45**, 4002 (1992).
- [32] D. M. Manley, R. A. Arndt, Y. Goradia and V. L. Teplitz, Phys. Rev. D **30**, 904 (1984).
- [33] M. Benmerrouche, N. C. Mukhopadhyay and J. F. Zhang, Phys. Rev. D **51**, 3237 (1995).
- [34] V. Crede *et al.* [CB-ELSA Collaboration], Phys. Rev. Lett. **94**, 012004 (2005).
- [35] O. Bartalini *et al.* [The GRAAL collaboration], Eur. Phys. J. A **33**, 169 (2007).

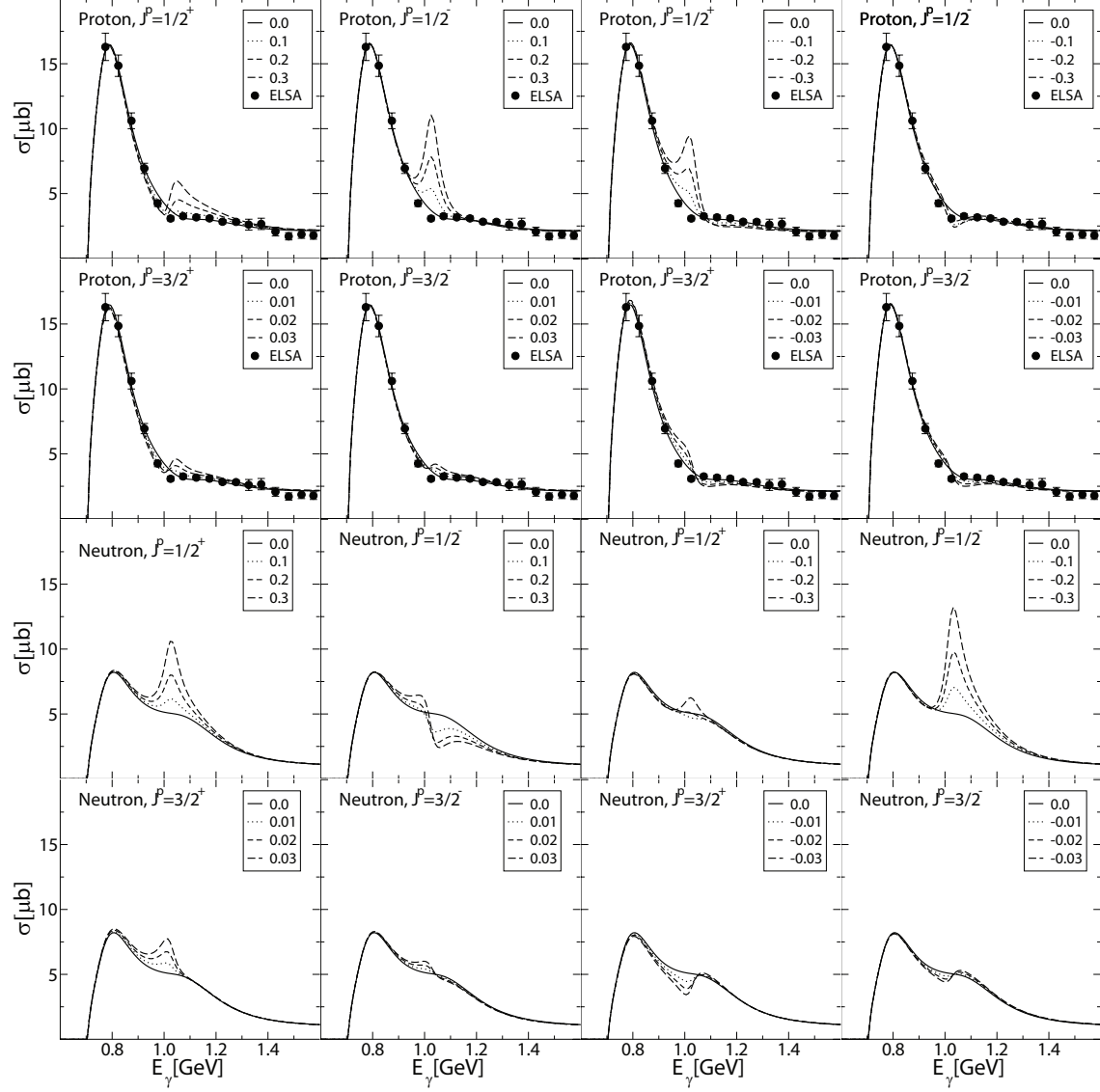


FIG. 2: Total cross sections for the proton (first and second rows) and neutron (third and fourth rows) as functions of the photon-laboratory energy in the laboratory frame.

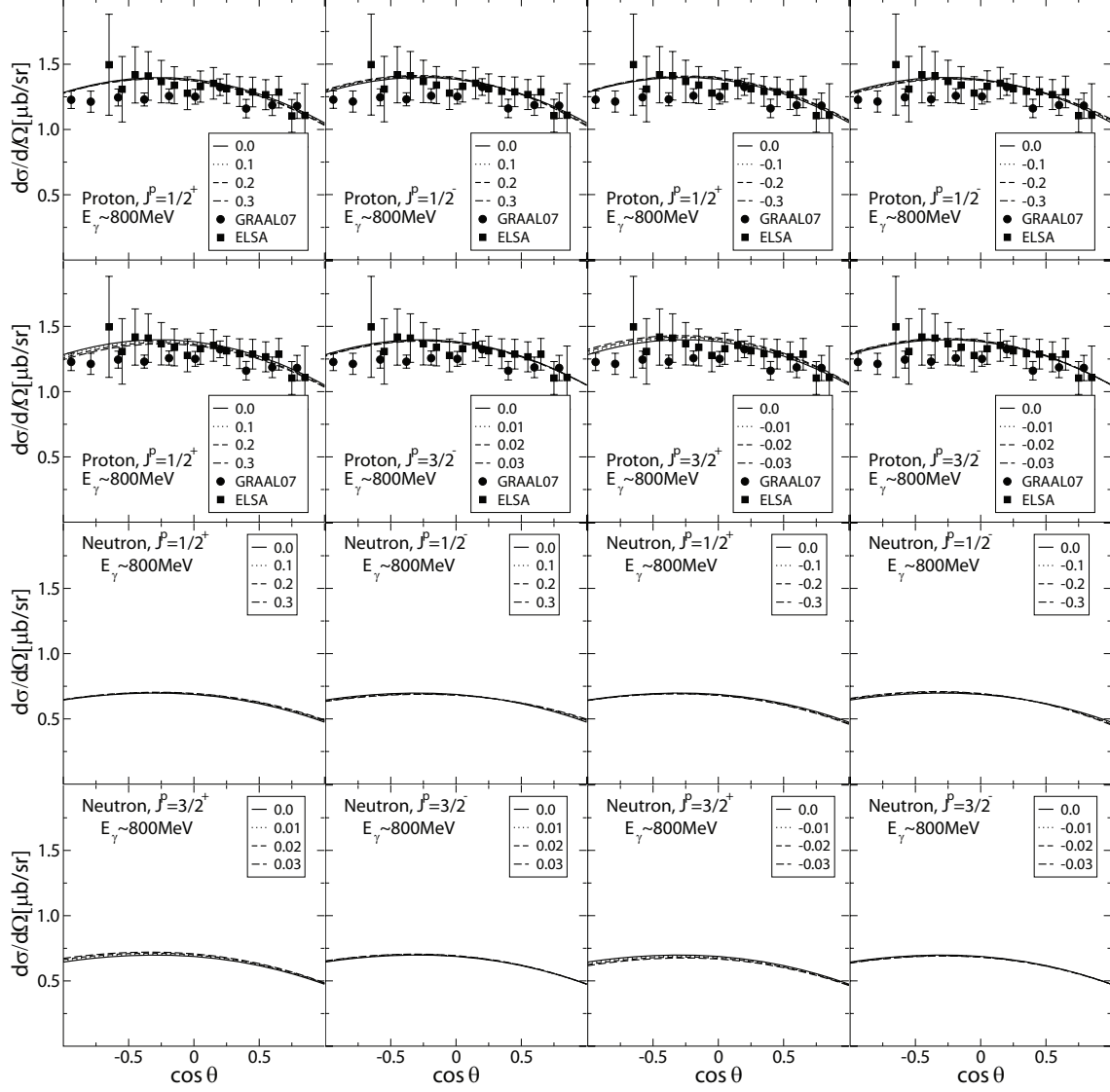


FIG. 3: Differential cross sections as functions of the scattering angle in the center of mass system  $\theta$  at  $E_\gamma \approx 800$  MeV for the proton (first and second rows) and neutron (third and fourth rows).

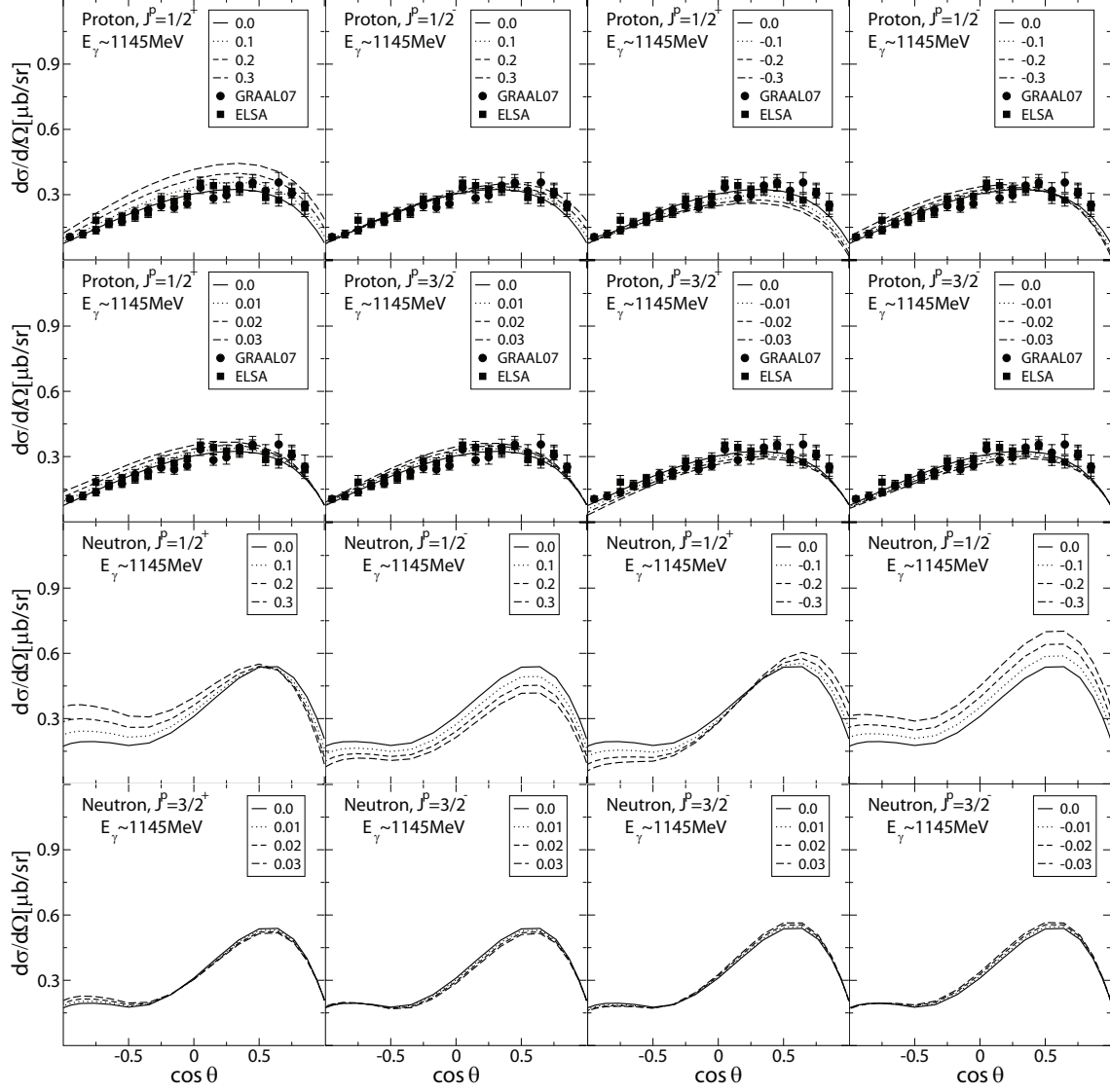


FIG. 4: Differential cross sections as functions of the scattering angle in the center of mass system  $\theta$  at  $E_\gamma \approx 1145$  MeV for the proton (first and second rows) and neutron (third and fourth rows).

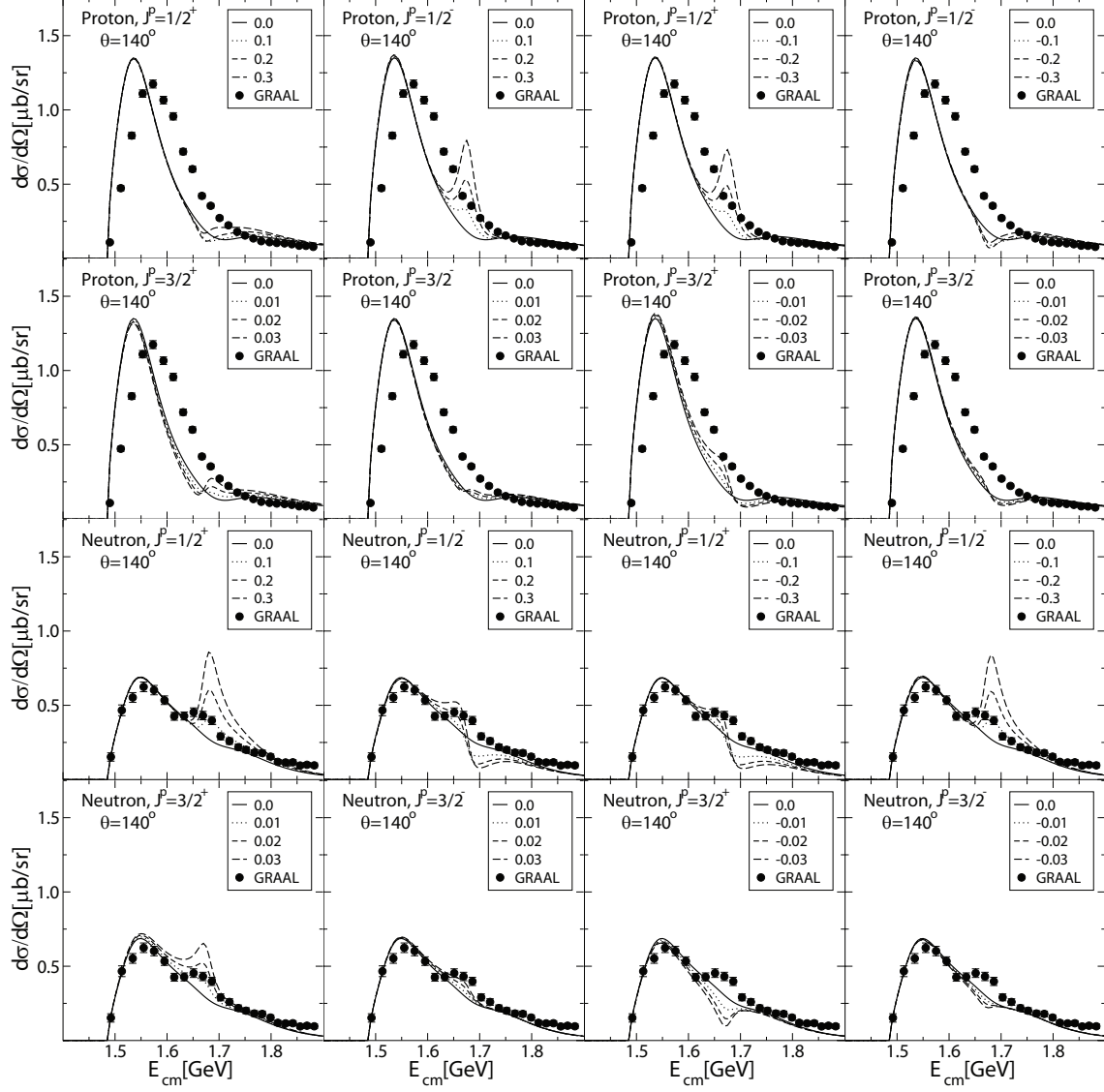


FIG. 5: Differential cross sections as functions of the photon energy at  $\theta \approx 65^\circ$  for the proton (first and second rows) and neutron (third and fourth rows).

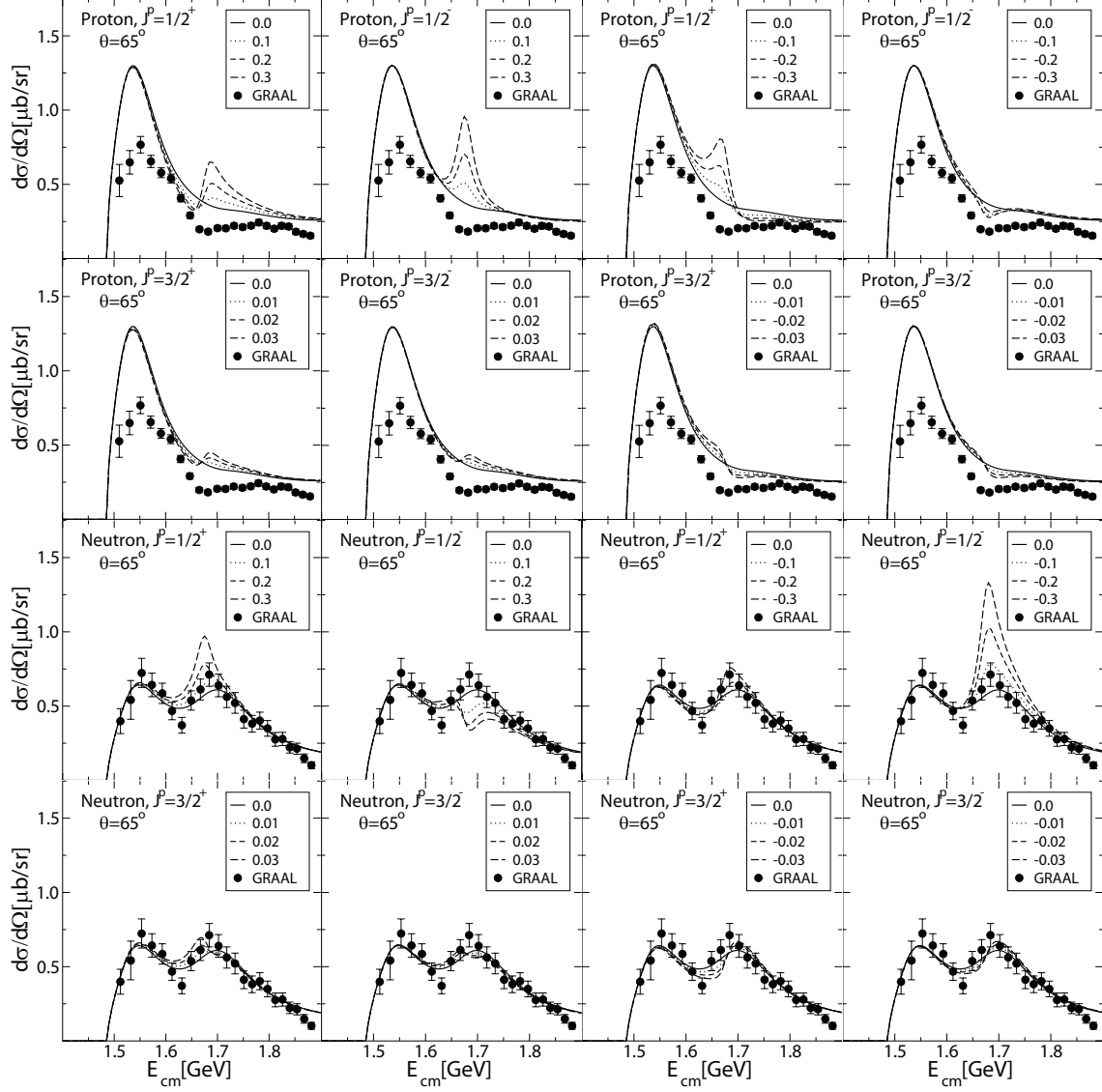


FIG. 6: Differential cross sections as functions of the photon energy at  $\theta \approx 140^\circ$  for the proton (first and second rows) and neutron (third and fourth rows).



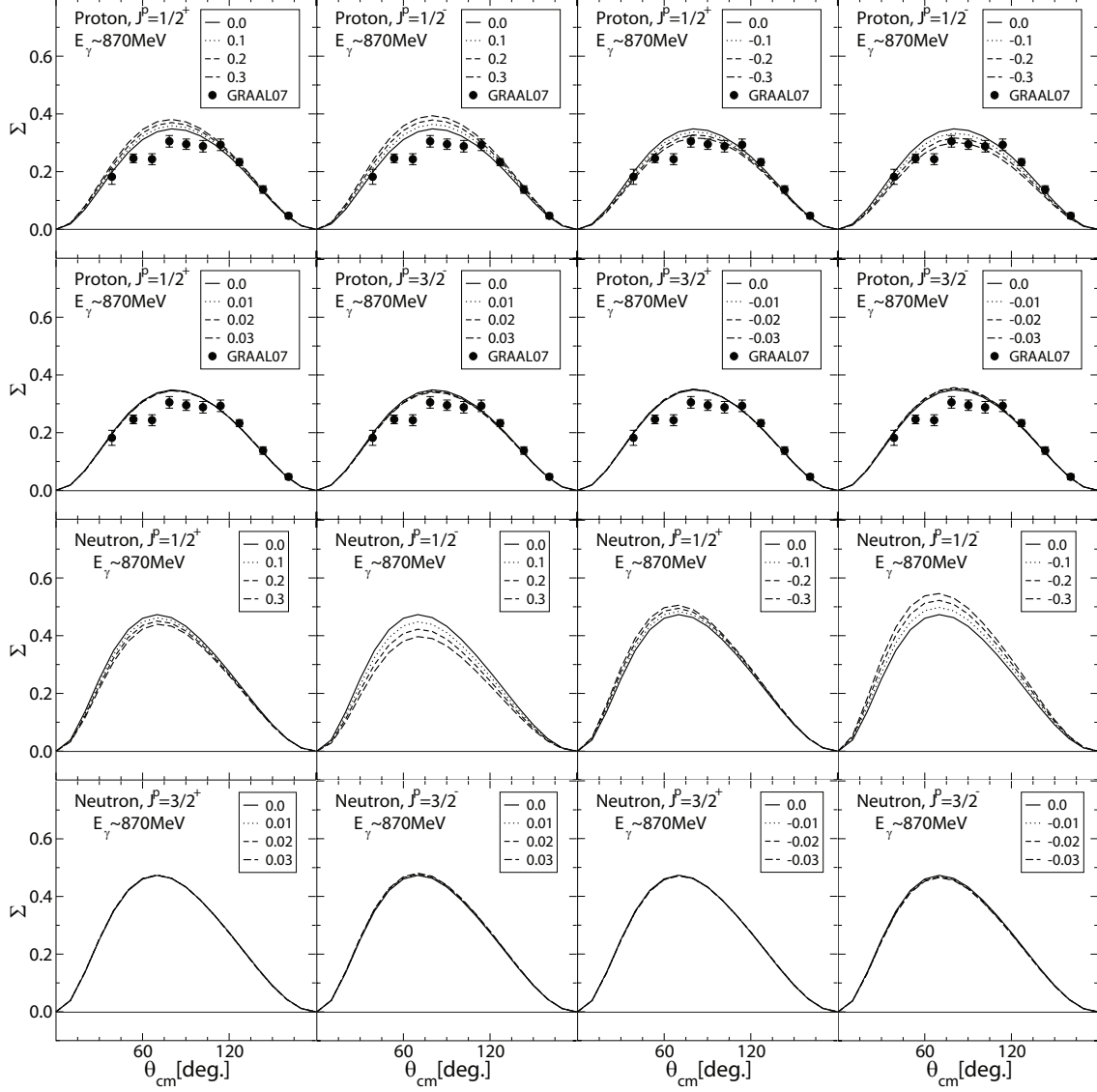


FIG. 7: Beam asymmetries as functions of the scattering angle in the center of mass system  $\theta$  at  $E_\gamma \approx 870$  MeV for the proton (first and second rows) and neutron (third and fourth rows).

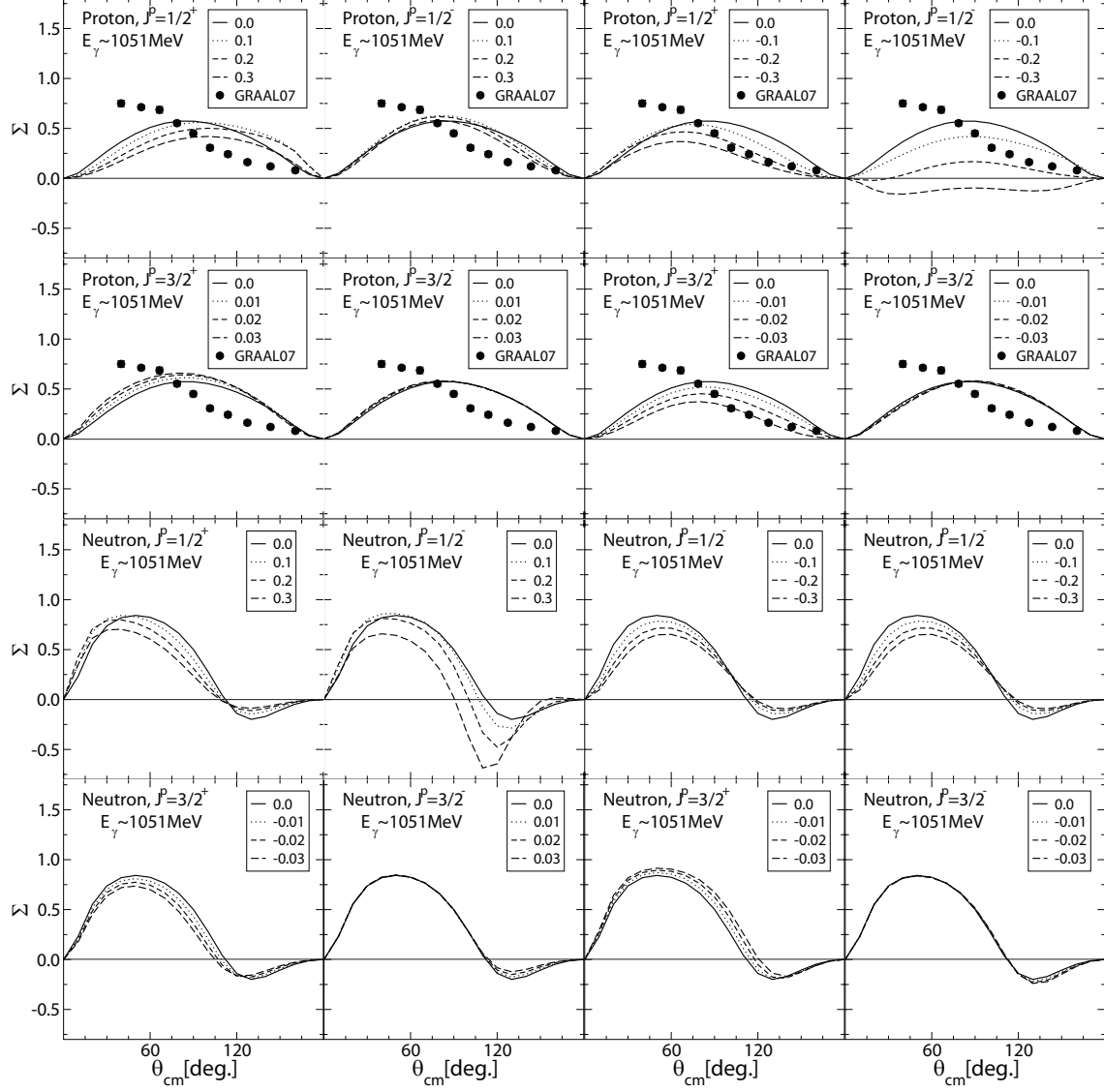


FIG. 8: Beam asymmetries as functions of the scattering angle in the center of mass system  $\theta$  at  $E_\gamma \approx 1051$  MeV for the proton (first and second rows) and neutron (third and fourth rows).